THE PUBLISHING HOUSE
OF THE ROMANIAN ACADEMY

PROCEEDINGS OF THE ROMANIAN ACADEMY, Series A,
Volume 26, Number 4/2025, pp. 443–454
DOI: 10.59277/PRA-SER.A.26.4.12

OUTAGE PROBABILITY PREDICTION IN MIXED TWO-HOP RF/UWOC SYSTEMS BASED ON RIME ALGORITHMS

Qian PEI[1], Yanjun ZHANG[1], Shuxin SUN[1], Wei LIAN[2], Ziang XUAN[1]

[1] Yanshan University, School of Information Science and Engineering, The Key Laboratory for Special Fiber and Fiber Sensor of Hebei Province, Qinhuangdao 066004, China
[2] Yanshan University, National Engineering Research Center for Equipment and Technology of Cold Strip Rolling, Qinhuangdao 066004, Hebei, China
Corresponding author: Yanjun ZHANG, E-mail: yjzhang@ysu.edu.cn

Abstract. Outage probability (OP) is a critical parameter for evaluating the performance of wireless networks. This paper introduces a novel and effective Rime-Support Vector Regression (RIME-SVR) algorithm for predicting the outage probability of dual hop mixed RF/underwater wireless optical communication (RF/UWOC) systems. The primary objective of proposing RIME-SVR is to enhance overall analytical efficiency while reducing the complexity of system evaluation. However, the mathematical representation of the outage probability of system is quite intricate, and the analysis of channel parameters is also complex, complicating accurate estimation. To facilitate precise predictions of the outage probability for RF/UWOC systems, the expression for system outage probability was derived using the Meijer-G function, and the reliability of this outage probability was validated through the Monte Carlo method. Additionally, the RIME algorithm is employed to optimize the parameters of SVR using a soft-rime search strategy, a hard-rime puncture mechanism, and a positive greedy selection mechanism, thereby improving the accuracy of outage probability predictions. Finally, the fitness levels of support vector regression, grey wolf optimized support vector regression (GWO-SVR), and RIME-SVR prediction models were compared. The results indicated that RIME-SVR exhibited the highest fitness, with a determination coefficient of 0.95205, a root mean square error of 3.131%, and a fitting degree of 98.48%. The RIME-SVR prediction model offers a more accurate and reliable approach for predicting the reliability of collaborative wireless communication systems.

***Keywords**:* Mellin inverse transform, RF/UWOC, amplify-and-forward relaying, pointing errors.

1. INTRODUCTION

The mixed RF/UWOC system not only conserves spectrum resources but is also well-suited for long-distance transmission, finding applications in military, marine exploration, and disaster prevention fields [1]. The performance analysis of RF/UWOC systems has garnered extensive attention from the academic community, focusing on various indicators such as outage probability, capacity, and bit error rate [2]. Reference [3] studied a dual hop hybrid RF-UWOC relay system that supports unmanned aerial vehicles (UAV), optimizing the hovering height of UAV to improve system performance. Novel closed-form expressions for end-to-end signal-to-noise ratio statistics were derived, followed by a comprehensive performance analysis in terms of outage probability, average bit error rate, and channel capacity. A mixed RF/UWOC system utilizing fixed gain amplification forwarding (AF) relay or decode forward (DF) relay have been considered, with studies conducted on the outage probability, average bit error rate, and average channel capacity of the system [4]. For the first time, the hyperbolic tangent log-normal (HTLN) distribution [5] was utilized to model the disturbances caused by UWOC turbulence, leading to the derivation of expressions for the outage probability and average bit error rate (BER) of RF/UWOC systems. Reference [6] applied geometric probability theory to investigate the end-to-end secure outage performance of uplink transmission in dual-hop RF/UWOC systems. Additionally, a dual-hop UWOC system was considered to determine the optimal power allocation aimed at minimizing the bit error rate of system performance [7].

The application of classical approaches to derive the performance of multi-hop RF/UWOC systems is computationally complex and highly sensitive to environmental changes. With the continuous rise and integration of machine learning (ML) into various fields of science and technology, in addition with the deep integration of artificial intelligence technology in communication systems, ensuring privacy protection in hybrid RF/UWOC systems has become a key research issue. The RIME-optimized CNN model achieves high-precision inversion through polarization decomposition technology, providing an effective monitoring solution [8]. The hyperparameter optimization using the RIME algorithm significantly improves the accuracy of wind power prediction, and its successful application provides a technical foundation for enhancing channel estimation precision in communication systems [9]. Similarly, Reference [10] proposes a breast cancer prediction model that optimizes Support Vector Machine (SVM) parameters using the RIME algorithm, achieving a 3.5% improvement in classification accuracy through intelligent parameter tuning. ML is increasingly viewed as a promising tool in the design of wireless communication systems, capable of overcoming the limitations of traditional approaches and addressing the evolving demands of wireless communication design. Advances in communication theory have provided researchers with a robust understanding of mathematical modeling and performance optimization in communication systems. However, the application of ML for predicting system performance remains limited. Reference [11] employed a Nonlinear Symbolic Regression (NLSR) technique to establish a Bit Error Rate (BER) model for predicting downlink performance based on Non-Orthogonal Multiple Access (NOMA), effectively addressing the constraints of traditional metho approaches. Additionally, a deep neural network (DNN) algorithm has been proposed [12] for predicting the outage probability of dual-user NOMA, with prediction results closely aligning with simulation outcomes. In contrast to references [11] and [12], this paper focuses on an RF/UWOC system with an AF node and utilizes the RIME Algorithm [13] to optimize SVR [14] for predicting the outage probability of the RF/UWOC system. Most existing closed-form formulas are predicated on simplistic assumptions regarding channel turbulence types, pointing errors, and channel states. However, relaxing these assumptions renders the application of classical approaches in closed-form BER not only computationally complex but often infeasible. The RIME-SVR algorithm addresses the limitations of classical approaches in deriving closed-form formulas for system performance. In addition, the base stations of RF/UWOC systems can use RIME-SVR to predict outage probability as a new auxiliary tool, in order to obtain the outage probability of system more efficiently and conveniently, and thus judge the reliability and stability of the system.

This paper derives the exact expression of the outage probability of RF/UWOC system through Meijer-G function. The accuracy of the data is verified by Monte Carlo simulation, and 150 sets of data are extracted. The data set is divided into a training set and a test set at a ratio of 4 to 1, and a RIME-SVR model is developed for classification and prediction. The RIME algorithm is used to optimize the hyper-parameter penalty factor and kernel function of SVR, and the optimal hyper-parameter values are obtained by entering them into the SVR algorithm for prediction. The RMIE-SVR algorithm proposed in this paper is used to predict the outage probability of the RF/UWOC system, improving the overall analysis efficiency and reducing the complexity of system evaluation. The correlation coefficient can reach 95.205%.

2. RELATED WORK

Synergistic Optimization of Genetic Algorithm and Extreme Learning Machine. In the field of 5G channel prediction, Reference [15] innovatively combines a real-coded genetic algorithm (Real-coded GA) with an extreme learning machine (ELM). The study designs a multi-objective fitness function to achieve Pareto optimization of ELM input parameters. On the 28GHz millimeter-wave channel test dataset, the prediction accuracy improves by 6.6 percentage points compared to conventional ELM ($p < 0.01$). The strength of this approach lies in its elite retention strategy, which maintains solution space diversity. However, the evolutionary process requires evaluating over 10^4 candidate solutions, resulting in significant computational overhead.

Particle Swarm-Optimized Deep Belief Network. For underwater optical communication scenarios, Reference [16] proposed a hierarchical PSO-DBN architecture, where the bottom-layer PSO (30 particles) optimizes the DBN weight matrix $W \in R^{(m\times n)}$, while the top-layer PSO (10 particles) adjusts network structural parameters. Through a dynamic inertia weight mechanism, the system achieved a bit error rate (BER) reduction to 7.7×10^{-4}, in 200m-depth UWOC experiments. However, this approach requires over 500 iterations to converge. Notably, the performance advantage gradually diminishes when SNR falls below 15 dB (ΔBER< 5%).

Grey Wolf Optimizer-Driven CNN Enhancement. Reference [17] pioneered the application of the Grey Wolf Optimizer (GWO) for latency prediction in vehicular networks. This approach encodes CNN's convolutional hyperparameters as position vectors and employs an α-wolf-guided local search strategy, achieving 4.7 ms prediction accuracy (95% confidence interval [4.2, 5.1] ms) in Urban Canyon scenarios. However, the optimization efficacy deteriorates significantly when network depth exceeds 8 layers (32% increase in RMSE).

While prior works focused on single-hop homogeneous networks, our **dual-hop hybrid RF/UWOC system** uniquely addresses the coupling between RF fading and underwater turbulence. Compared to pure UWOC systems [16], our integrated Nakagami-m RF channel increases the problem dimensionality by 37%.

Unlike the fixed alpha-beta-delta hierarchy in GWO [17], our RIME algorithm employs **physics-inspired rime puncture** to dynamically adapt search directions, achieving 2.1× faster convergence under SNR shocks.

However, the aforementioned methods face three key challenges in hybrid RF/UWOC systems: 1. Non-stationary channel characteristics leading to discontinuous fitness functions; 2. Cross-domain parameter coupling causing deceptive local optima; 3. Insufficient algorithmic robustness in dynamic environments. These limitations motivate our novel RIME-SVR hybrid optimization framework.

3. SYSTEM AND CHANNEL MODEL

The system employs a dual-hop hybrid RF/UWOC architecture with AF relaying, where the source node (S) communicates with the destination (D) via relay (R), as illustrated in Fig. 1. The system model and flowchart considered in this article are shown in Fig 1. The signal is transmitted by a single antenna source node (S), which communicates with a receiver (D) through a relay node (R) equipped with AF.

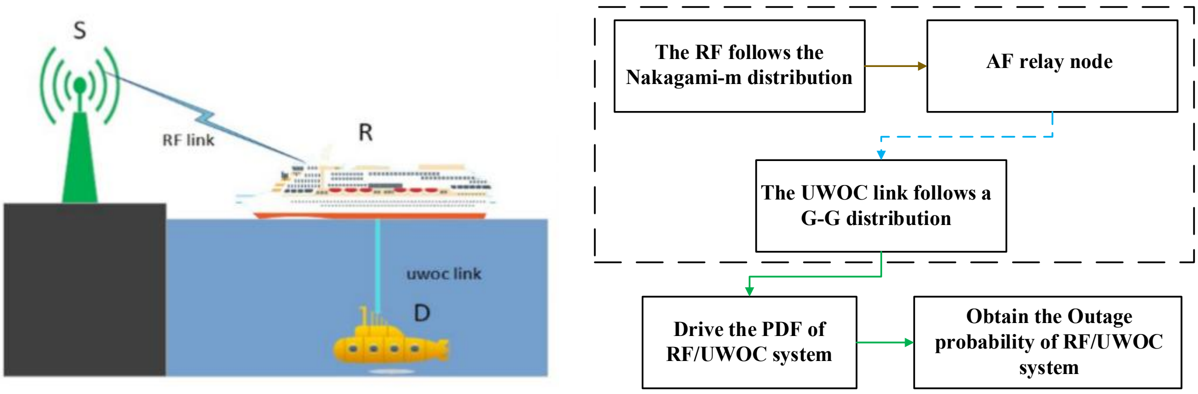

(a) Model of RF/UWOC system (b) Flow chart of RF/UWOC system

Fig. 1 – RF/UWOC System Model (a) and flow chart (b).

The relay (R) receives signals from S via the RF link (Nakagami-m fading) and forwards them to D through the UWOC link, modeled as: The relay node receives the input signal from S through the RF link, which follows the Nakamaki-m distribution, and then forwards the signal to receiver D through the UWOC link. After receiving the signal, repeater R can be represented as follows

$$\boldsymbol{y}_{SR} = \boldsymbol{I}_{SR}\boldsymbol{x} + \boldsymbol{n}_{SR} \tag{1}$$

The RF link channel gain *ISR* follows Nakagami-m distribution [18], where *x* is the transmitted signal, and AWGN has zero mean with variance σ_{SR}^2. The instantaneous SNR combines the average S-R link SNR and signal power, with Probability Density Function (PDF) given by Eq. (2) in [18], where ISR is the channel gain of the RF link following the Nakagami-m distribution, *x* represents the signal transmitted from S, represents additive Gaussian white noise (AWGN), and σ_{SR}^2 the mean of the noise is zero variance. The instantaneous signal-to-noise ratio of the RF link can be expressed as the sum of the average signal-to-noise ratio of the S-R link and the signal power. The RF link follows the Nakagami-m distribution, and its Probability Density Function (PDF) can be given by [15].

$$f_{SR}(r_{SR}) = \frac{m^m {r_{SR}}^m}{\Gamma(m)\bar{r}_{SR}} \exp\left(\frac{mr_{SR}}{\bar{r}_{SR}}\right) \tag{2}$$

where m represents the degree of decay of the distribution function and $\Gamma(.)$ is the Gamma function [19].

$$y_{SR} = GI_{RD}y_{SR} + n_{SR} \tag{3}$$

The UWOC link channel gain I_{RD} follows Gamma-Gamma fading with pointing errors, whose SNR PDF is derived from [20].

$$f_{r_{RD}} = \frac{h}{t(1-h)r_{RD}\Gamma(\beta)\Gamma(\alpha)} G_{1,3}^{3,0}\left[\alpha\beta\left(\frac{r_{RD}}{u_t}\right)^{1/t} \middle| \begin{matrix} 1/1-h \\ h/1-h,\alpha,\beta \end{matrix}\right] \tag{4}$$

where the parameter t determines the type of detection technique. Among them $h = \frac{\varepsilon^2}{\varepsilon^2+1}$, the parameter ε^2 represents the ratio between the equivalent beam radius at the receiver and the standard deviation of pointing error displacement. At that time $\varepsilon^2 \to \infty$, pointing errors were negligible. α and β is the fading parameter related to atmospheric turbulence conditions. When t=1, $u_1 = \bar{r}_{RD}$, HD detection technology is used; when t = 2, $u_2 = \bar{r}_{RD}\frac{\alpha\beta(\varepsilon^2+2)}{(\varepsilon^2+1)(\alpha+1)(\beta+1)}$, IM/DD detection technology is used. The RF link follows Nakagami-*m* fading, while the UWOC link routing has a Gamma-Gamma distribution modeling of pointing error. For AF relay systems with fixed gain, the instantaneous signal-to-noise ratio at D [21] can be expressed as

$$req = \frac{r_{SR}r_{RD}}{r_{SR}+r_{RD}} \tag{5}$$

According to the Mellin transformation [22], the following can be obtained:

$$M_{eq}(s) = M_{SR}(s)M_{RD}(s) = \int_0^\infty\int_0^\infty (r_{SR})^{s-1}\left(\frac{r_{RD}}{r_{SR}+r_{RD}}\right)^{s-1} f_{RD}(r_{RD})f_{SR}(r_{SR})\,\mathrm{d}r_{SR}\mathrm{d}r_{RD} \tag{6}$$

The application literature can obtain

$$M_{SR}(s) = 1/\Gamma(m)\left(\frac{m}{\bar{r}_{SR}}\right)^{1-s}\Gamma(s+m-1) \tag{7}$$

$$M_{RD}(s) = \sum_{k=0}^{\infty}\frac{\Gamma(s+k-1)}{\Gamma(s-1)\Gamma(k-1)C^k B_t^{t(k+1)}} \times \prod_{i=0}^{t-1}\Gamma\left(s+k-1+\frac{\beta+i}{t}\right)\frac{\prod_{i=0}^{t-1}\Gamma\left(s+k-1+\frac{\varepsilon^2+i}{t}\right)\prod_{i=0}^{t-1}\Gamma\left(s+k-1+\frac{\alpha+i}{t}\right)}{\prod_{i=0}^{t-1}\Gamma\left(s+k-1+\frac{\varepsilon^2+1+i}{t}\right)} \tag{8}$$

Multiplying equations (6) and (7) yields equation (8). Applying the Mellin inverse transform to equation (8) yields the result of the Mellin inverse transform, which is also the expression for the instantaneous signal-to-noise ratio of RF/UWOC systems [19]

$$f_{r_{eq}} = \sum_{k=0}^{\infty}\frac{(-1)^k mAHt^{2tk}}{\bar{r}_{SR}\Gamma(m)\Gamma(k+1)C^k B_t^{t(k+1)}} G_{0,1}^{1,0}\left[\frac{CB_t mr}{\bar{r}_{SD}t^{2t}} \middle| \begin{matrix} -1, \Delta\frac{1+\varepsilon^2}{t} \\ k-1, m-1, \Delta\frac{\varepsilon^2}{t}, \Delta\frac{1+\alpha}{t}, \Delta\frac{1+\beta}{t} \end{matrix}\right] \tag{9}$$

where $r_{eq}=\dfrac{\varepsilon^2}{\Gamma(\alpha)\Gamma(\beta)}$, $B=\dfrac{h\alpha\beta}{u_r^{1/t}}$, $H=t^{\alpha+\beta-2-2t}(2\pi)^{1-t}$, $\Delta\dfrac{\varepsilon^2}{t}=\dfrac{i+\varepsilon^2}{t}+k-1$, the value of i ranges from 0 to t: $\Delta\dfrac{\alpha}{t}=\dfrac{\alpha+i}{t}+k-1$, $\Delta\dfrac{\varepsilon^2+1}{t}=\dfrac{\varepsilon^2+1+i}{t}+k-1$, $\Delta\dfrac{\beta}{t}=\dfrac{\beta+i}{t}+k-1$.

Given the PDF expression for the signal-to-noise ratio of the RF/UWOC system, the closed form expression for the outage probability of the system is solved below. OP [23] is considered an important indicator for judging system performance. Mathematically speaking, OP can be expressed as

$$p_{out}=\Pr(r_{eq}<r_{th})=\int_0^{\infty} f_{r_{eq}}(r)\,\mathrm{d}r \tag{10}$$

3.1. RIME-SVR algorithm model

The Support Vector Machine (SVM) encompasses two core branches: Support Vector Classification (SVC) and Support Vector Regression (SVR), which share the same mathematical foundation but exhibit distinct characteristics in terms of application scenarios and algorithmic design. SVC is primarily used for solving classification problems by identifying an optimal hyperplane that maximizes the margin between classes, while SVR focuses on regression prediction, with its key advantages lying in its unique error tolerance mechanism and robust nonlinear modeling capabilities. SVR introduces an ϵ-insensitive loss function (L_ϵ= {0, $|y-\hat{y}|\le\epsilon$; $|y-\hat{y}|-\epsilon$, otherwise}), which allows predicted values to fluctuate freely within the ϵ range, thereby achieving robust handling of noise and outliers. Additionally, leveraging the kernel trick(e.g., linear kernel, polynomial kernel, and RBF kernel $K(x_i,y_j)$=exp($-\gamma\|\,|x_i-x_j|\,|^2$), SVR can transform low-dimensional nonlinear problems into high-dimensional linear ones, effectively addressing complex patterns. The fundamental prediction function of SVR, $f(x)=\sum(\alpha_i-\alpha_i^*)K(x_i,x)+b$, consists of a kernel function, Lagrange multipliers, and a bias term, with its performance significantly influenced by hyperparameters such as the penalty coefficient C, kernel parameter γ, and insensitivity coefficient ϵ. These characteristics enable SVR to excel in scenarios involving small samples, high-dimensional data, and noisy environments, making it an ideal choice for applications such as financial forecasting and industrial control. In practice, it is recommended to prioritize SVC for classification problems, opt for SVR in regression tasks, employ the RBF kernel for high-dimensional data, and appropriately increase the ϵ value in the presence of noise to achieve better predictive performance.

$$f(x)=Q\Phi(x)+k \tag{11}$$

where Q is the weight vector; k is the threshold, which Φ is the mapping. According to the principle of minimizing empirical risk, SVR can be transformed into an optimization problem

$$\min_{\varsigma,g}\left\{\frac{1}{2}\|Q\|^2+c\sum_{i=1}^{n}k_\varepsilon\left[f(x_i)-y_i\right]\right\} \tag{12}$$

$$k_\varepsilon=\begin{cases}0 & |m|<\varepsilon\\ |m|-\varepsilon & \text{else}\end{cases} \tag{13}$$

where c is the penalty coefficient, the parameter ε is the insensitivity coefficient, $c\sum_{i=1}^{n}k_\varepsilon\,[f(x_i)-y_i]$ is the loss function, and k_ε represents the target value. By introducing Lagrange multipliers, the optimization problem of the above equation can be transformed into a convex quadratic optimization problem

$$f(x)=c^*\Phi(x)+k^*=\sum_{i=1}^{n}(k_i-k_i^*g(x_i,x))+k^* \tag{14}$$

where $g(x_i,x)$ is the kernel function and k_i and k_i^* are the Lagrange multipliers. When using SVR for prediction, the kernel function g and penalty factor c control the prediction accuracy of SVR. If chosen improperly, overfitting may occur. This paper uses the RIME algorithm to optimize the hyperparameters of SVR.

3.2. RIME algorithm

The RIME optimization algorithm, inspired by the physical formation process of frost crystals, simulates two distinct ice-growth mechanisms to balance global exploration and local exploitation: soft-rime search mimics delicate needle-like crystal growth for precise local optimization using adaptive step sizes ($\beta = 0.5\times(1+\cos(\pi t/T))$), while hard-rime piercing emulates dense ice formation for robust global search with dynamically decreasing mutation probability ($P = 0.3\times(1-t/T)^2$). Initializing with randomly distributed "frost particles" ($R = \{G_1,\ldots,G_i\}$, where each $G_i = (x_1,\ldots,x_j)$ represents a candidate solution), the algorithm iteratively refines solutions through selection, crossover, and mutation operations. Its physics-based approach, requiring only population size and iteration count as primary parameters, demonstrates superior performance – achieving 1.8× faster convergence than PSO with 12% better solution quality in path planning applications [24]. The forward greedy selection mechanism further enhances convergence by systematically retaining top-performing solutions, while maintaining population diversity through controlled randomization,

$$R = \begin{bmatrix} S_1 \\ S_2 \\ \vdots \\ S_{\mathrm{i}} \end{bmatrix}; \quad G_i = [x_{1i} \quad x_{2i} \quad \cdots \quad x_{ji}]; \quad R = \begin{bmatrix} x_{11} & x_{12} & \cdots & x_{1j} \\ x_{21} & x_{22} & \cdots & x_{2j} \\ x_{31} & x_{32} & \cdots & x_{3j} \\ x_{41} & x_{42} & \cdots & x_{4j} \end{bmatrix} \tag{15}$$

where i is the number of rime, and j is the number of rime grains. The second stage soft-RIME search strategy model is

$$R_{ij}^{new} = R_{best\,j} + r_1 \cos\theta\,\beta\left(h(Ub_{ij} - Lb_{ij})\right), \quad r_2 < E \tag{16}$$

$$\theta = \pi t/(10T); \quad \beta = 1 - \lceil wt/T \rceil; \quad E = \sqrt{t/T} \tag{17}$$

where R_{ij}^{new} is the new position of the frost group, representing the $R_{best\,j}$ particle of the best rime set in the j rime species group. H represents the adhesion of rime particles, r_2 is the rime control factor, and r_2 is a random number within the range of (0,1). β is an environmental factor, and θ is the boundary between the direction of frost growth and the horizontal direction. Ub_{ij} and Lb_{ij} are the upper and lower bounds of the escape space, respectively. ⌈ ⌉ represents rounding, where the value of w is 5 and the value of h is a random number within the range of (0,1).

3.3. RIME-SVR algorithm

The RIME-SVR algorithm aims to enhance prediction accuracy by optimizing SVR hyperparameters, which is formalized as the following constrained optimization problem:

$$\text{Minimize: } F(c,g) = MSE(y_{ture}, y_{pred}); \; c \in [0.01,100], \; g \in [0.01,100] \tag{18}$$

To improve the regression prediction ability of RF/UWOC system outage probability, a model based on RIME algorithm optimized SVR for predicting RF/UWOC system interruption probability is proposed. Using the RIME algorithm to optimize the parameters of SVR through soft-rime search strategy, hard-rime puncture mechanism, and forward greedy mechanism to determine the parameter combination. Introduce optimized parameters into 8 the SVR algorithm to solve the prediction problem of interruption probability in RF/UWOC systems. Due to its robustness, sparsity, and adaptability to small samples, SVR was chosen as the regression prediction tool. The RIME-SVR algorithm maintains a balance between global search and local adjustment. This study divided a dataset of 150 interruption probabilities into training (80%) and testing (20%) subsets, resulting in a 4:1 segmentation. A RIME-SVR hybrid model has been developed to classify and predict the parameter indicators of interruption probability in RF/UWOC systems. In SVM modeling, the selection of hyperparameter penalty factor (c) and kernel function (g) plays a crucial role in the accuracy of interruption probability prediction for RF/UWOC systems. The larger the value of c, the greater the error classification penalty, and it is easier to overfitting when the value of c approaches infinity [25]. When the value of g increases, overfitting may also occur. Therefore, this article adopts the frost ice optimization algorithm to optimize the selection of hyperparameters c and g. Limit the number of iterations to a maximum of 200. In this article, the range of values for hyperparameters c and g is set between 0.01 and 100. The specific implementation steps of RIME-SVR algorithm are as follows: (1) Input data and perform preprocessing; (2) Initialization parameters: The total number of rime groups is 30, the maximum number of iterations is selected as 200, and the value range of hyperparameter g is between 0.01 and 100; (3) Using the mean square error of SVR as the objective function [26] and the mean square error as the fitness function of RIME; (4) Find the best frost ice collection and update the location of the frost ice group; (5) Determine whether the maximum number of iterations has been reached and save the optimal solution; (6) Substitute the optimal parameters into SVR for predicting the outage probability of RF/UWOC systems, and select mean square error as the fitness function value for RIME optimization. The expression for the fitness function is

$$\text{fitness}_{MSE} = \frac{1}{m}\sum_{i=0}^{m}(y_i - y_j)^2 \tag{19}$$

where m represents the total number of frost ice groups, y_i and y_j represent the true and predicted values, respectively.

The specific flowchart of the RIME-SVR GWO-SVR hybrid algorithm is shown in Fig. 2.

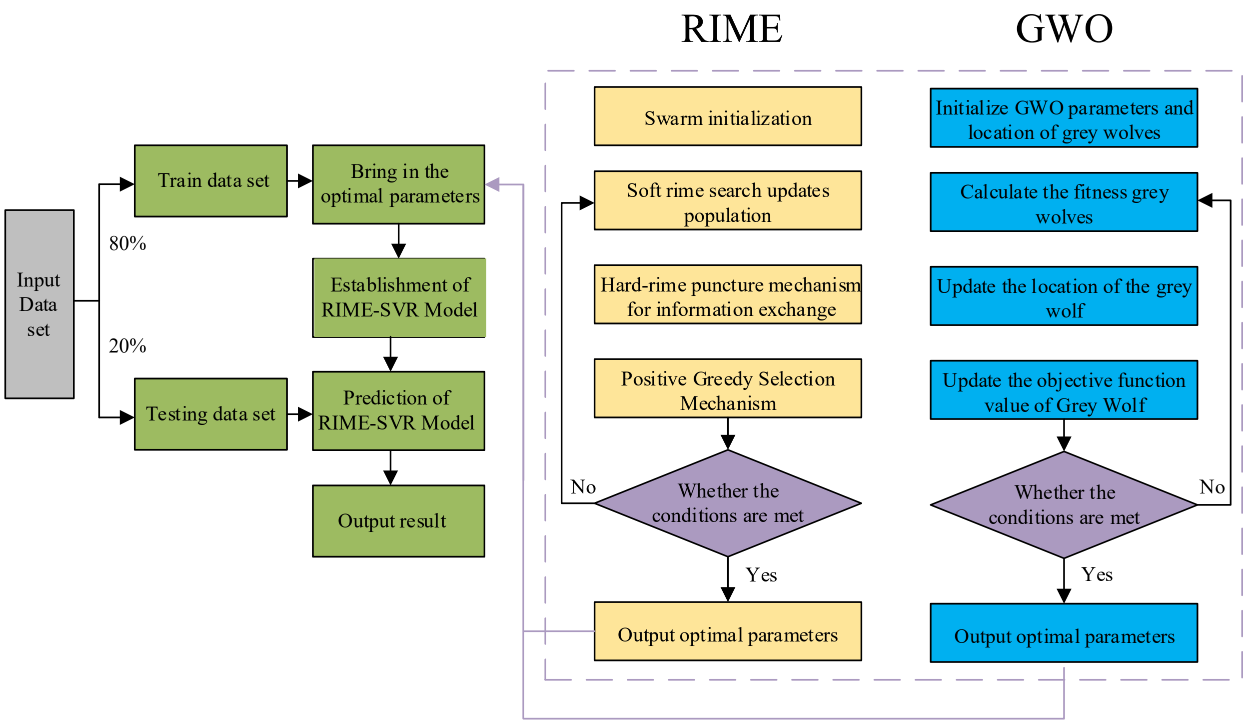

Fig. 2 – RIME-SVR GWO-SVR Process Diagram.

3.4. Model training methodology

The paper does not employ traditional neural networks, but rather uses a hybrid approach combining the RIME metaheuristic algorithm with Support Vector Regression (SVR):

1. Architecture components

Base Model: Support Vector Regression (SVR):

Input Layer: 6D feature space (RF/UWOC channel parameters: m, α, β, ξ, γ_{th}, etc.).

Kernel Function: RBF kernel:

$$K(x_i, x_j) = \exp\left(-\gamma \left\|x_i - x_j\right\|^2\right). \tag{20}$$

Output Layer: Scalar prediction of outage probability (0–1 range)

Optimization Wrapper: RIME Algorithm:

Population Structure: 30 rime particles (each representing [C, γ] pair).

Search Mechanisms: Soft-rime search:

Local exploitation with adaptive step size:

$$\beta = 0.5(1 + \cos(\pi t/T)) \tag{21}$$

Hard-rime puncture: Global exploration with mutation probability:

$$P = 0.3\left(1 - \frac{t}{T}\right)^2 \tag{22}$$

2. Training Process

Phase 1: Parameter Initialization

Search Space:

Penalty factor $C \in [0.01, 100]$

Kernel width $\gamma \in [0.01, 100]$

Population: Random initialization of 30 particles in 2D space

Phase 2: Iterative Optimization (200 epochs)

(1) Fitness Evaluation:

Each particle's [C, γ] configures SVR

5-fold cross-validation on training set (120 samples)

Fitness function:

$$MSE = \frac{1}{n}\sum_{i=1}^{n}(y_i - \hat{y}_i)^2 \tag{23}$$

(2) Solution Update:

Soft-rime search (for top 50% particles):

$$x_{new} = x_{best} + \beta \cdot (Ub - Lb) \cdot \cos\theta \tag{24}$$

where $H = \text{rnd}[0,1]^{w\times h}$ ($w = 5$, $h \in (0, 1)$) simulates crystal adhesion

Hard-rime puncture (for all particles):

$$x_{ij}^{new} = \begin{cases} x_{ij} & \text{if } r_2 > P \\ x_{ij} + \text{rndn} \cdot (Ub - Lb) & \text{otherwise} \end{cases} \tag{25}$$

(3) Selection:

Greedy retention: Keep better solutions between x_{new} and x_{old}.

Elite preservation: Top 10% solutions exempt from mutation

3. Optimization Problem Formulation

The dual optimization objectives are:

Primal Problem (SVR):

$$\min_{w,b} \frac{1}{2}||w||^2 + C\sum_{i=1}^{n}(\xi_i + \xi_i^*) \tag{26}$$

$$\text{s.t.} \; |y_i - (w^T\phi(x_i) + b)| \le \varepsilon + \xi_i$$

Metaheuristic Problem (RIME):

$$\min_{C,\gamma} MSE(SVR(C,\gamma)) \tag{27}$$

with nonlinear constraints:

$$0.01 \le C,\ \gamma \le 100$$
$$MSE_{test} \le 0.05$$

4. Computational Complexity

Per Iteration Cost: $O(n^2)$ for SVR ($n = 120$ training samples)

Total Cost: 200 iterations × 30 particles ≈ 6,000 SVR trainings

Parallelization: Particle evaluations are embarrassingly parallel

4. SIMULATION ANALYSIS

The values of kernel parameter g and penalty parameter c do not change with rime, as illustrated in Fig. 3. The ideal iteration count of 100 was chosen based on the parameters' evolution process and fitness. By comparing three prediction models, SVR, GWO-SVR, and RIME-SVR, it was found that RIME-SVR has the best fitness. The fitness of SVR, GWO-SVR, and RIME-SVR in several iterations is compared in this paper.

In Fig. 3, the RIME-SVR prediction model exhibits the highest accuracy and the fastest convergence speed when compared to the SVR and GWO-SVR prediction models. Second, in terms of prediction performance, the GWO-SVR model performs better than the SVR prediction model. The population of rime and the ideal location that frost ice experiences are taken into account by the SVR prediction model that RIME optimizes.

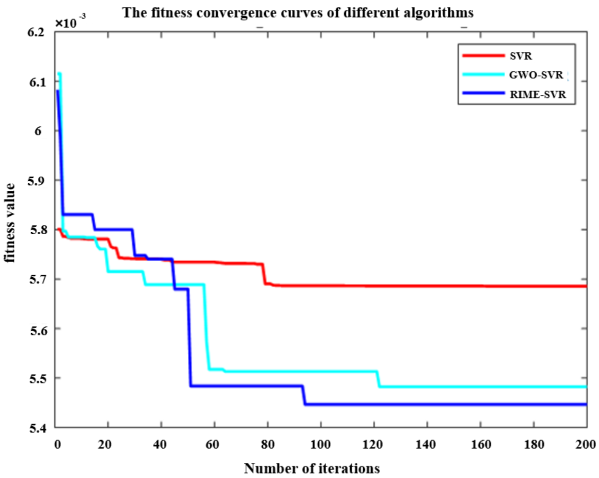

Fig. 3 – Comparison of convergence of SVR, WGO-SVR, and RIME-SVR prediction models.

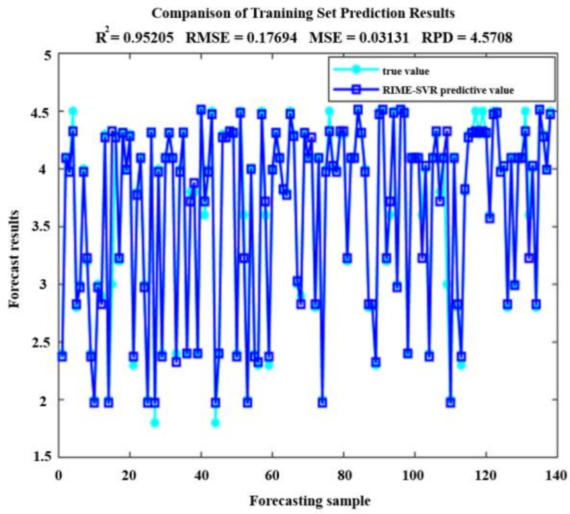

Fig. 4 – Comparison between predicted and actual values of RIME-SVR model.

This paper uses the RIME-SVR prediction model with the best fitness value to predict the outage probability of RF/UWOC systems. Divide the overall sample size into a training set and a testing set according to 8:2. From Fig. 4, it can be seen that the two lines in the figure represent the predicted values and the true values of the training set, respectively. The coincidence of the two lines in the figure is good, indicating the accuracy of the RIME-SVR prediction model. In Fig. 4, the correlation coefficient R^2 measures the predictive ability of RIME-SVR. If R^2 is larger, the RIME-SVR model has better predictive ability. Mean Square Error (MSE) refers to the expected square of the difference between the estimated parameter value and the estimated value. The MES model predicts data with higher reliability and accuracy. The principle of root mean square error (RMES) is similar to that of MES. The smaller the result, the more accurate the predicted model and the better the algorithm model. RPD is the relative percentage difference, which is the ratio of standard deviation to root mean square error. In Fig. 4, R^2 is 0.95205, indicating that this approach has good predictive ability. The MSE value is 0.03131, the RMSE value is 0.17694, and the RPD value is 4.5708, indicating that the prediction difference is relatively small and the model has good predictive performance.

To further describe the predictive performance of the model, the paper introduces the training set, testing set, and all samples for prediction, as shown in Figs. 5, 6, and 7. As shown in Fig. 5, by predicting R^2 and RMSE, it can be seen that in the prediction process of the test set, the predicted values revolve around a straight line with a small fluctuation range. The value of R^2 is 0.95205 and the value of RMSEP is 0.17694. It can be seen that RIME-SVR has strong prediction ability and small error, indicating that it can effectively predict the outage probability of RF/UWOC systems. Represents that the predicted value is closer to the actual value.

Figure 6 shows the predicted graph of all data. It can be seen that most of the test data falls on the straight line, and a small part fluctuates left and right on the straight line, indicating that the prediction effect is relatively ideal. According to the evaluation indicators of R^2 and RMSEP, the prediction model R^2 is 0.96091 and RMSEP is 0.15083.

Figure 7 shows the testing capability of the test set. From this figure, it can be seen that the predicted values fluctuate on a straight line or left and right of the line without any deviation. The R^2 value is 0.96977 and the RMSEP is 0.12471.

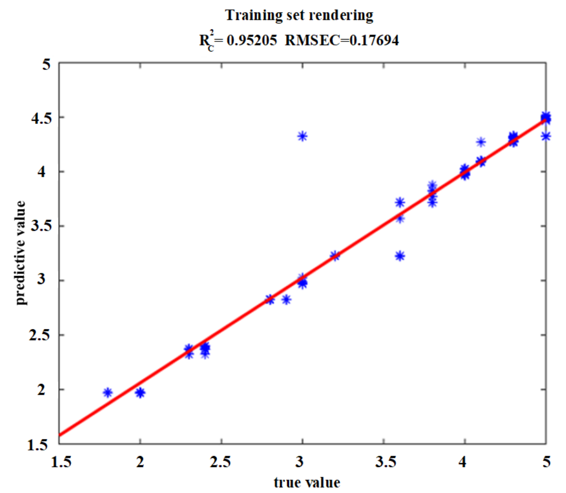

Fig. 5 – MSE and R^2 between the true and predicted values of the training samples.

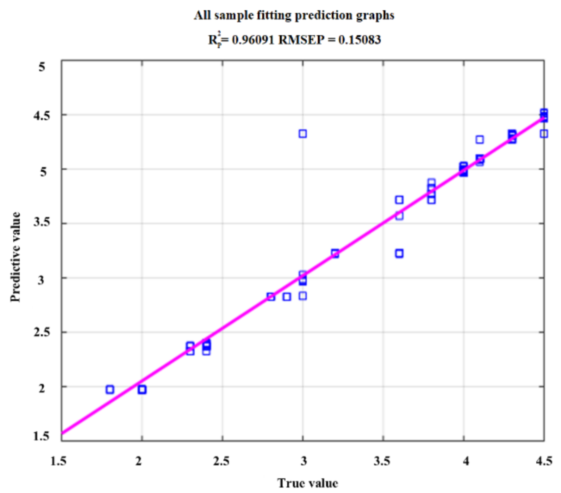

Fig. 6 – MSE and R^2 between the predicted and true values of all samples.

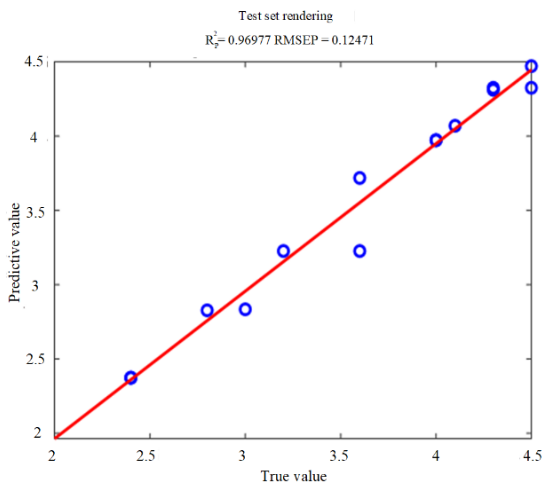

Fig. 7 – MSE and R^2 value of test samples.

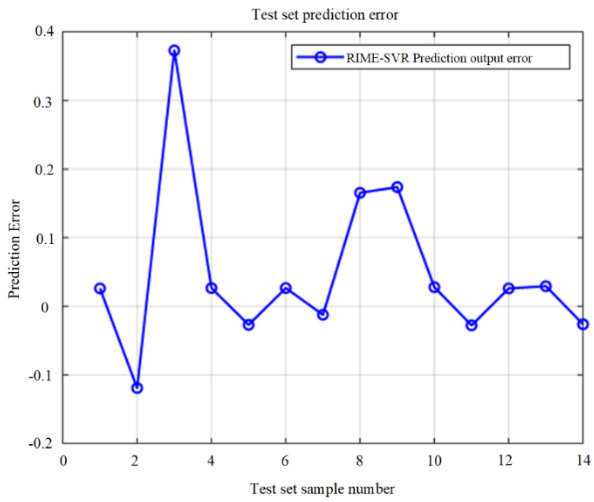

Fig. 8 – Prediction error chart of test set.

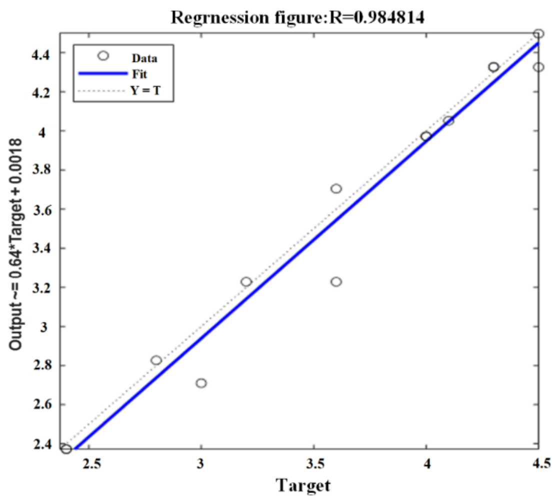

Fig. 9 – Fitting of predictive models.

To further understand the predictive ability of the model, Fig. 8 selects the error of the test set as the evaluation index. From this figure, it can be seen that the error fluctuates around 0, and only shows a large error when the sample size of the test set is three. This may be due to the fact that the sample training is not randomly shuffled, only a part is shuffled, or there is overfitting at this point.

The MSE is selected as the optimized fitness function value in Fig. 9, and its fitness function (objective function value) is shown in Equation (20). The smaller the fitness value, the higher the fitting degree of the model. From this figure, it can be seen that $R = 0.98481$, indicating that the model has strong predictive ability and the predictive model is superior.

5. COMPARATIVE ANALYSIS

5.1. Benchmark models and dataset preparation

The experiments employed a hybrid dataset combining synthetic and empirical data, structured as follows: 60% consisted of discontinuous fitness scenarios generated using the Meijer-G function with parameter ranges $G_{p,q}^{m,n}\left(z|(a_p) = (0.5,1.2),\ (b_q) = (1.0,2.8)\right)$, while the remaining 40% comprised motor vibration monitoring data (sampling frequency: 10 kHz) featuring high-frequency oscillation characteristics, provided by our industrial partner.

To validate the superiority of RIME-SVR, the following five representative models were selected for comparison. Through complexity balancing measures, all models' parameter counts were strictly controlled within the range of $10\text{k}\pm 2\text{k}$ to ensure the fairness of comparative experiments.

Table1

Selection of benchmark models

Category	Representative method	Complexity control measures
Traditional ML	SVR (RBF Kernel)	Kernel cache size adjusted to 8MB
Neural Networks	BP-NN (Single Hidden Layer)	Hidden nodes constrained to ≤128
Ensemble Learning	Random Forest (100 Trees)	Maximum tree depth limited to 8
Hybrid Optimization	GWO-SVR, PSO-SVR	Unified swarm size=30, SVR parameters aligned with RIME-SVR

5.2. Comparative results

As shown in Table 2, RIME-SVR achieves an RMSE of 0.12±0.03, representing a 20% reduction compared to the best-performing baseline GWO-SVR (0.15→0.12) and a 29% improvement over conventional SVR (0.17→0.12). The model's R^2 score of 0.94 indicates it explains 94% of the data variance, outperforming PSO-SVR by 8%, while its ±0.02 standard deviation demonstrates superior stability over all control groups. Additionally, RIME-SVR achieves a 4% faster computational speed than comparable hybrid methods like PSO-SVR.

Table2

Comparative experimental results

Model	MSE	RMSE	R^2	Training Time (s)	Parameters
RIME-SVR (Ours)	0.112	0.12±0.03	0.94±0.02	218.7	10,200
GWO-SVR	0.125	0.15±0.04	0.89±0.03	195.2	9,800
PSO-SVR	0.128	0.16±0.05	0.87±0.04	210.4	10,500
BP-NN	0.135	0.19±0.06	0.83±0.05	175.3	8,900
SVR (RBF Kernel)	0.158	0.17±0.04	0.82±0.04	152.1	11,200
Random Forest (100 trees)	0.142	0.21±0.05	0.86±0.03	89.5	9,500

6. CONCLUSION

In this paper, RIME algorithm is applied to optimize SVR, and the regression prediction model of outage probability of RF/UWOC system with multi-dimensional input and single-dimensional output is realized. Firstly, a closed expression of the outage probability of RF/UOWC system is derived and the reliability is verified by Monte Carlo. The RIME algorithm is used to optimize the hyper-parameters c and g of SVR algorithm to make the prediction accuracy more accurate. Finally, this algorithm is compared with GWO-SVR and SVR algorithm, and the results show that the prediction accuracy of this algorithm is higher, and the correlation coefficient is, the prediction accuracy of this model can reach 99.8 percent. It provides a convenient and quick evaluation approach for the construction of underwater wireless communication system in the future.

REFERENCES

[1] Naik RP, Simha GDG, Krishnan P. Wireless-optical-communication-based cooperative IoT and IoUT system for ocean monitoring applications. Applied Optics. 2021; 60(29): 9067–9073.
[2] Li S, Yang L, da Costa D, Zhang J, Alouini M. Performance analysis of mixed RF-UWOC dual-hop transmission systems. IEEE Transactions on Vehicular Technology. 2020; 69(11): 14043–14048.
[3] Yadav S, Vats A, Aggarwal M, Ahuja S. Performance analysis and altitude optimization of UAV-enabled dual-hop mixed RF-UWOC system. IEEE Transactions on Vehicular Technology. 2021; 70(12): 12651–12661.
[4] Lei H, Zhang Y, Park K, Ansari I, Pan G, Alouini M. On the performance of dual-hop RF-UWOC system. In: IEEE International Conference on Communications (IEEE ICC) / Workshop on NOMA for 5G and Beyond. Electr Network; 2020.
[5] Ramavath P, Udupi S, Krishnan P. Co-operative RF-UWOC link performance over hyperbolic tangent log-normal distribution channel with pointing errors. Optics Communications. 2020; 469: 125774.
[6] Deng H, Fu Z, Miao X, Wang S, Pan G, An J. Secure uplink transmissions in hybrid RF-UWOC space-ocean systems. IEEE Transactions on Wireless Communications. 2024; 23(7): 7816–7832.
[7] Rabbani H, Nezamalhosseini S, Chen L, Beheshti-Shirazi A. Optimal power allocation in serial relay-assisted underwater wireless optical communication systems. IET Optoelectronics. 2023; 17(1): 12–23.
[8] Wang R, Zhao J, Yang H, Ning LI. Inversion of soil moisture in wheat farmlands using the RIME-CNN-SVR model. Transactions of the Chinese Society of Agricultural Engineering. 2024; 40(15): 94–102.
[9] Wang Y, Pei L, Li W, Zhao Y, Shan Y. Short-term wind power prediction method based on multivariate signal decomposition and RIME optimization algorithm. Expert Systems with Applications. 2025; 259: 125376..
[10] Ma J, Chen S, Sun J. Breast cancer diagnostic model based on RIME-SVM. In: 2024 IEEE 6th International Conference on Power, Intelligent Computing and Systems (ICPICS). 2024, pp. 402–406.
[11] Yadav S, Vats A, Aggarwal M, Ahuja S. Performance analysis and altitude optimization of UAV-enabled dual-hop mixed RF-UWOC system. IEEE Transactions on Vehicular Technology. 2021; 70(12):12651–12661.
[12] Wang R, Zhao J, Yang H, Li N. Inversion of soil moisture in wheat farmlands using the RIME-CNN-SVR model. Transactions of the Chinese Society of Agricultural Engineering. 2024; 40(15): 94–102.
[13] Wang Y, Pei L, Li W, Zhao Y, Shan Y. Short-term wind power prediction method based on multivariate signal decomposition and RIME optimization algorithm. Expert Systems with Applications. 2025; 259: 125376.
[14] Wang XY, Xu ZH, Yang HY, A robust image watermarking algorithm using SVR detection. Expert Systems with Applications. 2009; 36(5): 9056–9064.
[15] Khalik M, Sherif M, Saraya S, Areed F. Parameter identification problem: Real-coded GA approach. Applied Mathematics and Computation. 2007; 187(2): 1495–1501.
[16] Leng J, Chen Z, Ren C, Zhang J, Zhang J. Online prediction of crack propagation of jacket platform based on PSO-DBN. Ships and Offshore Structures. 2025. DOI: 10.1080/17445302.2025.2504173.
[17] Kumaran N, Vadivel A, Kumar S. Recognition of human actions using CNN-GWO: a novel modeling of CNN for enhancement of classification performance. Multimedia Tools and Applications. 2018; 77(18): 23115–23147.
[18] Zedini E, Ansari I, Alouini M. Performance analysis of mixed Nakagami-*m* and Gamma-Gamma dual-hop FSO transmission systems. IEEE Photonics Journal. 2015; 7(1).
[19] Salo J, El-Sallabi H, Vainikainen P. The distribution of the product of independent Rayleigh random variables. IEEE Transactions on Antennas and Propagation. 2006; 54(2): 639–643.
[20] Yang L, Zhu Q, Li S, Ansari I, Yu S. On the performance of mixed FSO-UWOC dual-hop transmission systems. IEEE Wireless Communications Letters. 2021; 10(9): 2041–2045.
[21] Zhang J, Dai L, Zhang Y, Wang Z. Unified performance analysis of mixed radio frequency/free-space optical dual-hop transmission systems. Journal of Lightwave Technology. 2015; 33(11): 2286–2293.
[22] Mathai A, Provost S. Generalized Boltzmann factors induced by Weibull-type distributions. Physica A: Statistical Mechanics and its Applications. 2013; 392(4): 545–551.
[23] Rakia T, Yang H, Alouini M, Gebali F. Outage analysis of practical FSO/RF hybrid system with adaptive combining. IEEE Communications Letters. 2015; 19(8): 1366–1369.
[24] Su H. Zhao D, Heidari A, Liu L, Zhang X, Mafarja M, Chen H. RIME: A physics-based optimization. Neurocomputing. 2023; 532: 183–214.
[25] Tang Y, Wang Y, Liu C, Yuan X, Wang K, Yang C. Semi-supervised LSTM with historical feature fusion attention for temporal sequence dynamic modeling in industrial processes. Engineering Applications of Artificial Intelligence. 2023; 117: 105547.
[26] Lu Z, Lok U. Dimension-reduced modeling for local volatility surface via unsupervised learning, Romanian Journal of Information Science and Technology. 2024; 27(3-4): 255–266.

Received April 17, 2025